

## Preparation and Characterization of Equilibrium Adsorption-Prepared Molybdena-Alumina Catalysts

C. V. CACERES,<sup>\*,1</sup> J. L. G. FIERRO,<sup>\*,2</sup> A. LOPEZ AGUDO,<sup>\*</sup> M. N. BLANCO,<sup>†</sup>  
AND H. J. THOMAS<sup>†</sup>

<sup>\*</sup>*Instituto de Catalisis y Petroleoquímica, CSIC, Serrano 119, 28006 Madrid, Spain, and* <sup>†</sup>*Centro de Investigación y Desarrollo de Procesos Catalíticos (CINDECA), C 47, N° 257, 1900 La Plata, Argentine*

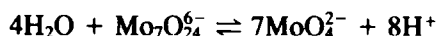
Received February 12, 1985; revised May 1, 1985

The preparation of molybdena-alumina catalysts was studied using an equilibrium adsorption method at 50°C in which the molybdenum anions from solution were adsorbed on the alumina surface at pH values between 5.70 and 7.70 near to its isoelectric point. In these experimental conditions a two-step adsorption isotherm was found, indicating that the loading of the carrier was very dependent on the solute concentration. By combining different characterization techniques, namely, temperature-programmed reduction and kinetics of reduction, reflectance spectroscopy, chemisorption of NO and O<sub>2</sub> probe-molecules, infrared spectroscopy of NO, and extraction by ammonia, it is shown that at low solute concentrations the Mo is highly dispersed, mostly as tetrahedrally coordinated (by oxygen ions) Mo species. However, poorer dispersion was found at intermediate and high solute concentrations. In this latter case, the combined use of chemisorption and extraction data indicated that on calcining at 500°C the surface of the carrier becomes populated with both tetrahedrally (monolayer) and octahedrally (small clusters) coordinated Mo-species. © 1985 Academic Press, Inc.

### INTRODUCTION

The importance of the concentration and pH of the impregnating solution in the preparation of molybdena-alumina catalysts has been recognized and used to explain the characteristics and behavior of the surface species of catalysts (1-8). A pioneer work about the genesis of molybdena-alumina catalysts was reported by Sonnemans and Mars (4). They found that the amount of Mo adsorption on the alumina surface is strongly dependent on the solution pH, it being higher at acidic pH than at basic pH. Afterward, Brunelle (9) and Parfitt (10) showed that ideas from colloidal chemistry can be applied, with certain restrictions, to the surface chemistry of oxides. In the particular case of alumina with an isoelectric point (IEP) in the range 6.0-8.0 (11), it will be either positively or negatively charged

when "impregnated" with ammonium heptamolybdate (AHM) solutions of pH lower or higher than the IEP, respectively. Moreover, in the AHM solutions the following ionic equilibrium occurs,



which means that the adsorption of octahedrally coordinated polymolybdate, Mo[O], ions should be favored by low pH, whereas at high pH the adsorption of the tetrahedrally coordinated, Mo[T], ions would be favored.

Many works have been repeatedly reported in the literature and disagreement exists concerning the coordination of Mo in molybdena-alumina catalysts. Several authors (12) have found it to be Mo[T], whereas others (1, 5, 8) have claimed both Mo[T] and Mo[O] symmetries, although most of all these preparations were made by the incipient wetness technique and occasionally the monolayer capacity was exceeded. However, when adsorption from

<sup>1</sup> On leave from CINDECA, C 47, N° 257, 1900 La Plata, Argentine; under a fellowship from CONICET.

<sup>2</sup> To whom correspondence should be addressed.

solution was performed at low AHM concentration (3, 6) a constant amount of Mo adsorbed was reached and a second plateau was only attained by using solute concentrations above such limit (13). In this latter case, it was established on the basis of X-ray diffraction patterns and diffuse reflectance spectra (DRS) that the first plateau is due to the formation of a molybdenum monolayer, mainly as Mo[T], whereas the second one is due to adsorption of polyanions (Mo[O]) which formed upon calcining three-dimensional MoO<sub>3</sub>-like crystallites. However, recent electrophoretic migration and Mo extraction results, with several series of molybdena-alumina catalysts prepared by different impregnation methods, have shown that Mo is present in both monolayer and multilayer forms, even at low Mo loading (14). Such characterization studies were, however, not applied to catalysts prepared by an equilibrium adsorption method, in which the solute in excess was removed before drying of the catalysts.

In view of the above, in the present work we report the characterization in detail of a series of oxidic molybdena-alumina catalysts and their corresponding ammonia-extracted molybdena-alumina samples by the combined use of several techniques, e.g., diffuse reflectance spectroscopy, temperature-programmed reduction (TPR), kinetics and extent of reduction by H<sub>2</sub>, chemisorption of O<sub>2</sub> and NO probe-molecules, and infrared spectroscopy of NO. Characterization of the molybdena-alumina catalysts, before and after Mo extraction by ammonia solution, provides very useful information for understanding the surface structure of such catalysts.

#### EXPERIMENTAL

**Preparation of the catalysts.** The support was a commercial  $\gamma$ -alumina,  $S_{\text{BET}}$  of 180 m<sup>2</sup> g<sup>-1</sup>, pore volume of 0.50 cm<sup>3</sup> g<sup>-1</sup>, ground and sieved to below 150  $\mu$ m. Catalysts were prepared by impregnation of the alumina powder with an aqueous solution of AHM (Merck, reagent grade) by the adsorption

from solution procedure. Alumina samples of 1.0 g were shaken in 4 cm<sup>3</sup> of a solution of known concentration (varying between 5 and 120 mg Mo cm<sup>-3</sup>) at 50°C for 20 h. The initial and final pH values for few preparations are summarized in Table 1. Then the solids were separated by centrifugation, dried at 110°C and calcined in air at 450°C for 15 h.

**Extraction of molybdenum.** Extraction of Mo by solubilization was carried out by treating 0.5-g samples with 120 cm<sup>3</sup> of a 3% ammonia (pH 12.6) solution for 0.5 h. The solubilized Mo was determined in the filtrate by atomic absorption spectrometry.

**TPR.** Temperature-programmed reduction by H<sub>2</sub> was performed by means of a Cahn microbalance. Samples (24.2 mg) were first heated at a rate of 240°C h<sup>-1</sup> in dry He (7.2 dm<sup>3</sup> h<sup>-1</sup>) up to 600°C and this temperature was kept constant until constant weight, this being followed by cooling to room temperature. Then the samples were contacted with H<sub>2</sub> (7.2 dm<sup>3</sup> h<sup>-1</sup>) and heated at a rate of 240°C h<sup>-1</sup> until a final temperature of 1000°C. Only derivative weight-temperature curves were considered in representations.

**Reduction experiments.** Reduction measurements were carried out in the same microbalance connected to a high-vacuum line and gas-handling system. Samples of 140 mg were first outgassed at room temperature and then the temperature was raised to 510°C, this temperature being maintained until constant weight. After

TABLE 1  
Variation of pH of the Mo Solutions during Impregnation

Solute concentration (mg Mo cm <sup>-3</sup> )	Initial pH	Final pH <sup>a</sup>
20	5.70	6.95
50	6.05	7.15
80	6.16	7.42
120	6.40	7.70

<sup>a</sup> After shaking mixtures for 20 h.

this, samples were contacted with  $40 \text{ kN m}^{-2} \text{ H}_2$  (99.999% purity) and the integral kinetic curves of reduction were recorded. A liquid-nitrogen temperature trap ( $-196^\circ\text{C}$ ) placed near the samples condensed the water produced in reduction. All experiments were carried out under isobaric conditions, as the dead volume of the microbalance was large as compared to the negligible  $\text{H}_2$  volume required for the reduction.

**NO and  $\text{O}_2$  chemisorptions.** NO and  $\text{O}_2$  adsorptions were effected on reduced catalysts. All the samples were reduced to a reduction degree  $\alpha = 0.92\text{--}0.95$  (the experimental weight loss was equal to the theoretical one assuming that  $\text{Mo}^{6+}$  is reduced to  $\text{Mo}^{4+}$ ), outgassed under dynamic high vacuum ( $\sim 10^{-3} \text{ N m}^{-2}$ ) at  $510^\circ\text{C}$  for 3 h and then cooled to  $-196^\circ\text{C}$ . When constant weight was attained,  $\text{O}_2$  ( $13.3 \text{ kN m}^{-2}$ ) was contacted with the catalyst. After equilibrium was reached the samples were outgassed until constant weight was attained to remove the physically adsorbed  $\text{O}_2$  fraction. Details of the procedure are given elsewhere (15). Afterward, the samples were outgassed under dynamic high vacuum at room temperature for 1 h and reduced again with  $\text{H}_2$  ( $40 \text{ kN m}^{-2}$ ) at  $510^\circ\text{C}$  until constant weight. Then they were outgassed under dynamic high vacuum at the same temperature for 3 h and cooled to room temperature. Very pure NO ( $4.4 \text{ kN m}^{-2}$ ), obtained by two freeze-thaw cycles at  $-196^\circ\text{C}$ , was contacted with the samples and the extent of chemisorption was measured as above.

**DRS and IR.** Diffuse optical reflectance spectra were recorded with a Varian Super Scan 3 spectrophotometer. Wafers of the catalysts and reference compound ( $\text{BaSO}_4$ ) were prepared by pressing the powdered materials at  $3 \times 10^3 \text{ kN m}^{-2}$ . The spectra were recorded in the wavelength region 200–500 nm. Infrared spectra were obtained with a Perkin-Elmer 682 spectrophotometer. Self-supporting wafers of the samples were prepared by pressing the

powdered catalysts between two mica sheets at  $2 \times 10^2 \text{ kN m}^{-2}$ ; final thickness was  $10.2\text{--}12.0 \text{ mg cm}^{-2}$ . The wafers were placed in a vacuum cell which allowed thermal treatment under dynamic vacuum of ca.  $1 \times 10^{-3} \text{ N m}^{-2}$ . These samples were outgassed under these vacuum conditions at  $510^\circ\text{C}$  for 1 h and subsequently reduced in  $\text{H}_2$  ( $40 \text{ kN m}^{-2}$ ) at the same temperature for 1 h. After this, they were outgassed for 2 h, cooled to room temperature, and contacted with  $4 \text{ kN m}^{-2} \text{ NO}$  for 0.5 h; the gaseous NO was then condensed at liquid-nitrogen temperature. In an additional experiment the 8.9%  $\text{Mo}/\text{Al}_2\text{O}_3$  catalyst was reduced at  $820^\circ\text{C}$  for 1 h, outgassed at this temperature for 2 h, cooled to room temperature, and then contacted with  $0.94 \text{ kN m}^{-2} \text{ CO}$  (99.998% purity). All spectra were recorded at room temperature.

## RESULTS AND DISCUSSION

### Adsorption Isotherm of Molybdenum

The adsorption isotherm of molybdenum at  $50^\circ\text{C}$  is given in Fig. 1. It is expressed as the Mo concentration on the support ( $C_i$ ) as a function of the solute concentration in equilibrium ( $C_f$ ). Exploratory kinetic mea-

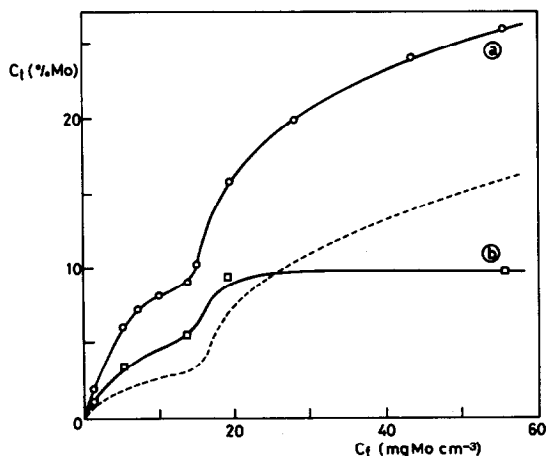


FIG. 1. (a) Molybdenum adsorption isotherm on  $\gamma\text{-Al}_2\text{O}_3$  after 20 h of equilibration for different initial solute concentrations. (b) Molybdenum adsorption isotherm obtained after extraction of catalysts of isotherm (a) by an ammonia solution ( $\text{pH} = 12.6$ ). Dashed line is difference isotherm (a) - (b).

surements indicated that after 2 h the Mo loading was essentially constant; however, a much longer time (20 h) was selected in order to be sure that equilibrium was attained (13).

The effect of the solute concentration on the equilibrium loading was found to be very important. As observed in Fig. 1, at concentrations below  $14 \text{ mg Mo cm}^{-3}$  the curve increased steeply, with an abrupt change of slope above such a concentration. However, the Mo-extracted preparations showed a virtually flat curve at solute concentrations above  $20 \text{ mg Mo cm}^{-3}$ ; below such a concentration the Mo loading was slightly lower than in the overall isotherm. The difference between both curves (dashed line) gave the Mo-extractable isotherm in which the majority Mo species must be Mo[O]. It is evident that the contribution of these species to the second ascending branch of the overall isotherm is very important. As the impregnation of the alumina with AHM was performed at lower pH values than the IEP of the alumina (Table 1), polyanions also became the adsorbed species and much more so at higher solute concentrations. Moreover, for these high solute concentrations a certain contribution of precipitation of a molybdate phase could take place. Upon drying these clusters remain intact, but some decomposition may occur during calcination to form multilayered  $\text{MoO}_3$  structures. This finding is also supported by the X-ray diffraction patterns of the noncalcined preparations which showed large interplanar spacing lines attributable to the presence of polyanions (or precipitated molybdate phase). This result is in good agreement with the observations made by Trifiro *et al.* (16) and by Shapiro *et al.* (17) who established that with increasing solute concentrations polyanions of increasing size are formed.

### Diffuse Reflectance Spectra

According to the literature (5, 12, 13), Mo[T] exhibits an absorption band at about

260 nm, whereas Mo[O] exhibits two bands, a characteristic one at about 320–350 nm and another at a wavelength similar to that of Mo[T].

From the diffuse reflectance spectra of the catalysts, the variation of the Kubelka–Munk functions determined at 350 and 260 nm, i.e.,  $F(R_\infty)_{350}/F(R_\infty)_{260}$ , with the Mo loading is shown in Fig. 2. On the basis that the scattering coefficient is almost constant for all the species and the Kubelka–Munk function for dilute systems is proportional to the concentration of absorbing species (18), the ratio  $F(R_\infty)_{350}/F(R_\infty)_{260}$  can be used as an approximate estimate of the relative concentration of Mo[O] to the total (Mo[T] + Mo[O]) one. Thus, Fig. 2 shows that the concentration of Mo[O] increased with increasing solute concentration. Two regions, which correspond to the two branches of the adsorption isotherm (Fig. 1), can be differentiated in Fig. 2. At Mo loadings above 10% the relative increase in polyanions, Mo[O], seems to be higher than at low Mo loadings, i.e., the adsorption of polyanions is strongly favored at high solute concentrations.

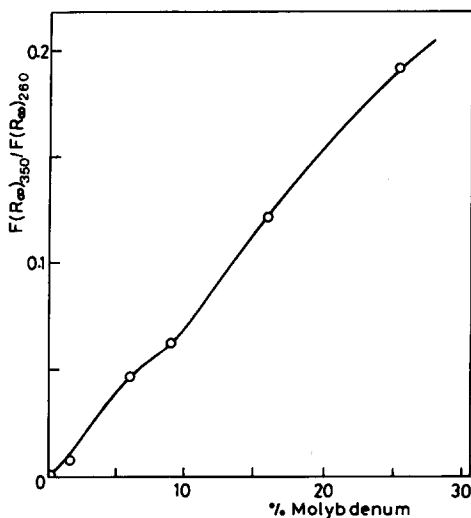


FIG. 2. Ratio of SKM functions (taken from the ultraviolet–visible reflectance spectra of  $\text{Mo}/\text{Al}_2\text{O}_3$  preparations given in Fig. 1) as a function of the Mo loading.

### TPR Profiles

The TPR patterns of Mo/Al<sub>2</sub>O<sub>3</sub> catalysts in their unextracted and extracted forms are given in Figs. 3a and b, respectively. The starting reduction temperatures as well as the temperatures at which the TPR maxima occur are summarized in Table 2. It can be seen from these data that the reducibility of the Mo/Al<sub>2</sub>O<sub>3</sub> catalysts is connected with the Mo loading. The starting reduction temperature decreases with increasing Mo loading, this effect being much smaller for the Mo-extracted preparations. For example, the 8.9% Mo/Al<sub>2</sub>O<sub>3</sub> catalyst started to be reduced at 316°C whereas the parent Mo-extracted one with 5.5% Mo started at 395°C. Notice also that for both unextracted and extracted catalysts with almost the same Mo loading the starting reduction temperature follows the same trend. This indicates not only that the interaction between the Mo species and the support is stronger at lower Mo loadings, but also that the degree of aggregation increases with increasing Mo loading, i.e., decreasing dispersion.

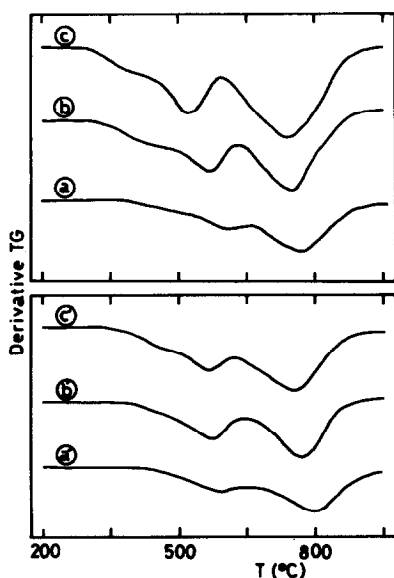


FIG. 3. TPR patterns of molybdena-alumina catalysts with varying Mo loadings: (a) 1.8%; (b) 8.9%; and (c) 25.6%. Mo-extracted catalysts whose final Mo loadings were (a') 1.1%; (b') 5.5%; and (c') 9.7%.

TABLE 2

TPR Parameters of Mo/Al<sub>2</sub>O<sub>3</sub> Catalysts

	Mo (%)	$T_{st}$ (°C)	$T_1$ (°C)	$T_2$ (°C)
Impregnated	1.8	380	590	770
	8.9	316	566	752
	25.6	302	515	740
Extracted	1.1	420	597	800
	5.5	395	570	774
	9.7	380	563	760

Complementary information is obtained from the two maxima ( $T_1$  and  $T_2$ ) observed on each TPR pattern. Although such maxima could be ascribed to the reduction of two well-defined Mo species whose reducibility is also different (19), it is more probably due to two separate steps in the reduction of Mo ions. It is well known that the reduction of Mo<sup>6+</sup> ions by H<sub>2</sub> at temperatures about 500°C gives preferentially Mo<sup>4+</sup>; however, a deeper reduction of such ions at temperatures above 650°C may progress up to metallic Mo. Thus, the  $T_1$  peak could arise from the first reduction step, whereas the  $T_2$  one could then be ascribed to a deeper reduction of the ionic Mo sites down to metallic Mo.

This last finding is supported by the infrared spectra obtained when CO was adsorbed on 8.9% Mo/Al<sub>2</sub>O<sub>3</sub> catalyst prereduced in H<sub>2</sub> at 510 and 820°C for 1 h (Fig. 4). CO was used as probe-molecule because it is less likely than NO to reoxidize metallic sites. CO chemisorption on the H<sub>2</sub>-reduced 8.9% Mo/Al<sub>2</sub>O<sub>3</sub> catalyst at 510°C shows bands at 2230 and 2185 cm<sup>-1</sup> typical of CO held on exposed Al<sup>3+</sup> sites (20) and on ionic Mo sites, probably Mo<sup>4+</sup> (but possibly Mo<sup>3+</sup> or Mo<sup>2+</sup>). After reduction at 820°C three bands at 2230, 2140, and 2045 (very strong) cm<sup>-1</sup> were observed. The assignment of the first two bands may be the same as for the catalyst reduced at 510°C, but the band at 2045 cm<sup>-1</sup> is usually considered to arise from CO typically held in lin-

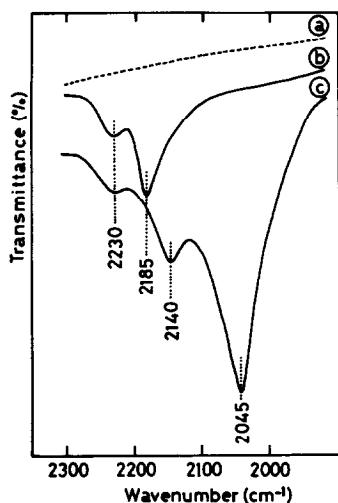


FIG. 4. IR spectra of CO chemisorbed on high-temperature  $H_2$ -reduced 8.9%  $Mo/Al_2O_3$  catalyst. (a) Background; (b) after contacting with  $0.94 \text{ kN m}^{-2}$  CO at room temperature on prereduced catalyst at  $510^\circ\text{C}$  for 1 h; and (c) after contacting with  $0.94 \text{ kN m}^{-2}$  CO at room temperature on prereduced catalyst at  $820^\circ\text{C}$  for 1 h.

ear configuration on fully reduced sites, i.e., on metallic Mo (21–23).

On this basis, it is concluded that the reduction of the catalysts proceeds in two steps, namely one at temperatures of ca.  $500^\circ\text{C}$  giving rise to partially reduced ionic Mo sites (majority  $Mo^{4+}$ ), and a second one at temperatures above  $650^\circ\text{C}$  producing fully reduced Mo sites. In addition, since both TPR peaks are very broad it is inferred that the heterogeneity of the surface must be important. The higher reduction temperatures indicate a stronger interaction of Mo at the alumina surface.

### Kinetics of Reduction

The kinetic reduction curves of two catalysts containing 6.1 and 25.6% Mo are given in Fig. 5a. For comparative purposes, the kinetic reduction curves of their parent Mo-extracted 3.5 and 9.7%  $Mo/Al_2O_3$  catalysts, respectively, are also included. In these kinetic curves the reduction degree ( $\alpha$ ) was represented as a function of time.  $\alpha$  was defined as the ratio of experimental to theoretical weight loss upon reduction. Theoret-

ical weight loss values were obtained by assuming that the overall  $MoO_3$  initially present in the catalysts is quantitatively reduced to  $MoO_2$ , namely for the reduction process  $MoO_3 \rightarrow MoO_2$   $\alpha$  is unity. Although this assumption is somewhat arbitrary, it allows to compare both the extent of reduction and the reduction rate at any time.

As can be observed, the time required to achieve a given value is greater for the samples with lower Mo loading but much greater for the Mo-extracted ones. This is in agreement with the TPR patterns presented above. In other words, in the same experimental conditions the reduction rate becomes faster when Mo loading increases.

The initial reduction rate at zero time ( $r_0$ )

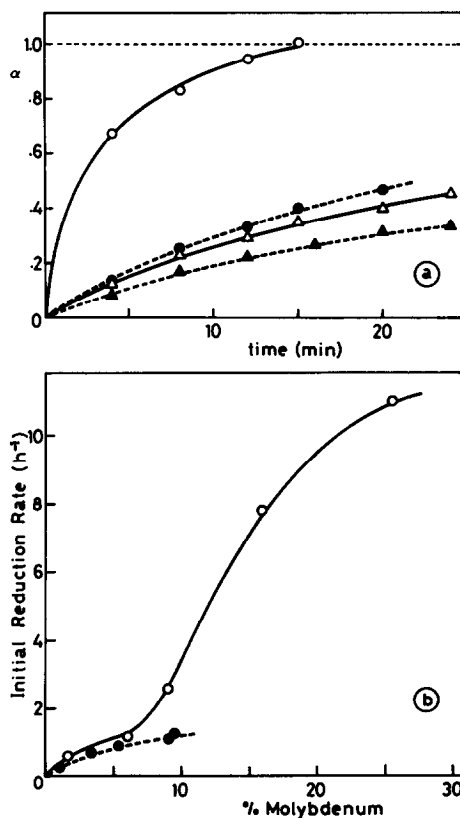


FIG. 5. (a) Kinetic reduction curves by  $H_2$  at  $510^\circ\text{C}$  of (○) 25.6%; and (△) 6.1%  $Mo/Al_2O_3$  catalysts; and their (●) 9.7%; and (▲) 3.5%  $Mo/Al_2O_3$  extracted ones, respectively. (b) Initial reduction rates ( $r_0$ ) as a function of Mo loading.

is another interesting kinetic parameter which reflects the relative ease of removal of the O atoms from the oxidic Mo species and, consequently, gives indirect information about the environment of Mo atoms. It was obtained from the integral kinetic curves of reduction fitted to a hyperbolic function and differentiated at zero time. The  $r_0$  values as a function of the Mo loading for both unextracted and extracted Mo/ $\text{Al}_2\text{O}_3$  catalysts are given in Fig. 5b. For the unextracted catalysts it is observed that  $r_0$  increases slowly with the Mo loading up to about 8% Mo, but increases rapidly at higher concentrations. However, for the Mo-extracted catalysts  $r_0$  increases also with Mo loading but rather slowly as compared to that of the unextracted preparations. These results would indicate that, at least, two different Mo species are present on the alumina surface, at low and high Mo loadings, respectively.

#### Infrared Spectra of NO

The infrared spectra of NO chemisorbed on both unextracted (Mo loading ranging between 1.8 and 25.6%) and extracted (Mo loading ranging between 1.1 and 9.7% Mo) Mo/ $\text{Al}_2\text{O}_3$  catalyst series are given in Figs. 6A and B, respectively. All spectra show two absorption bands at 1810 and 1710  $\text{cm}^{-1}$  assigned to the symmetric and antisymmetric NO fundamental stretching, respectively, of paired NO molecules held either as a dimer (24, 25) or as a dinitrosyl (26) on a surface Mo ion, probably  $\text{Mo}^{4+}$  or  $\text{Mo}^{3+}$  (27). It is interesting to note that bands at similar wavenumbers were observed for NO adsorbed on  $\text{H}_2$ -reduced Mo/ $\text{Al}_2\text{O}_3$  catalysts (24, 25, 27, 28) and thermally activated  $\text{Mo}(\text{CO})_6/\text{Al}_2\text{O}_3$  catalysts (26).

The relative intensity of the two bands is related to the angle  $\theta$  between the two N–O oscillators by the equation  $I_{\text{sym}}/I_{\text{anti}} = \text{ctg}^2(\theta/2)$ . The relative intensities, the angle  $\theta$ , and the full width at half maximum (FWHM) results for both unextracted and extracted Mo/ $\text{Al}_2\text{O}_3$  catalyst series are summarized in Table 3. We can see that the

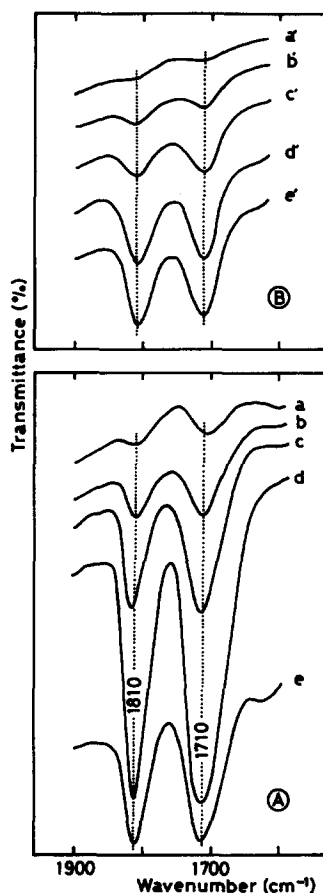


FIG. 6. (A) IR spectra of adsorbed NO at room temperature on partially reduced catalysts with different Mo loadings: (a) 1.8%; (b) 6.1%; (c) 8.9%; (d) 15.9%; and (e) 25.6%. (B) IR spectra of NO on partially reduced Mo-extracted catalysts with different Mo loadings: (a') 1.1%; (b') 3.5%; (c') 5.5%; (d') 9.5%; and (e') 9.7%.

angle  $\theta$  decreases slightly with increasing Mo loading for both series, whereas the FWHM shows an opposite trend. These differences can be explained in terms of the reduction degree of the catalysts. As already stated above, and in agreement with several investigators (1, 29–32), the Mo is present in both Mo[T] and Mo[O] environments. At 510°C the former species are resistant toward reduction, thus a lower amount of reduced Mo sites is expected to be present in the low-Mo-loading Mo/ $\text{Al}_2\text{O}_3$  catalysts and, consequently, NO adsorption should be lower. In this situation  $(\text{NO})_2$

TABLE 3  
Infrared Parameters for the Molybdenum (NO)<sub>2</sub>  
Adsorption Complexes

	% Mo	$I_{\text{sym}}/I_{\text{anti}}$	$\theta$ (°)	FWHM <sup>a</sup> (cm <sup>-1</sup> )
Unextracted	1.8	0.66	102	28
	6.1	0.68	101	30
	8.9	0.73	99	32
	15.9	0.81	96	34
	25.6	0.78	97	35
Extracted	1.1	0.63	102	—
	3.5	0.73	99	36
	5.5	0.70	100	37
	9.5	0.78	97	40
	9.7	0.78	97	40

<sup>a</sup> Band at 1810 cm<sup>-1</sup>.

dimers or nitrosyls may interact with other reduced ionic Mo neighbors, thus increasing the angle  $\theta$  between the two NO oscillators.

Another interesting point to note is the slightly broader bands for the dimers or nitrosyls on the Mo-extracted preparations. The broader bands for such catalysts indicate a wider adsorption site distribution due to a larger surface heterogeneity of the alumina compared to the adsorption sites in the unextracted Mo/Al<sub>2</sub>O<sub>3</sub> catalysts. Furthermore, it is interesting to observe in Fig. 6 that the band at 1710 cm<sup>-1</sup> is considerably broader than the one at 1810 cm<sup>-1</sup> (24, 25). It may be explained on this basis that the vibrational transition moment vector which is parallel to the surface will detect the surface inhomogeneities more effectively than the one which is perpendicular to the surface (symmetric vibration).

Figure 7 shows the integrated intensities of the band at 1710 cm<sup>-1</sup> of both unextracted and extracted Mo/Al<sub>2</sub>O<sub>3</sub> catalysts as a function of the Mo loading. As can be seen, the integrated intensity of the band in the unextracted catalyst series increases steeply with increasing Mo loading up to about 15% Mo and then markedly decreases. The reduction data given in Fig. 5a show that a higher reduced Mo ion expo-

sure exists in catalysts with high Mo loading than in those with low Mo loading. Therefore the observed decrease in the intensity of the NO band for high Mo loading cannot be explained in terms of a lower reduction degree. Peri (23) has suggested that the explanation may lie in the formation of aluminum molybdate during calcination, which might occur more readily when excess of Mo beyond the monolayer, interacting strongly with the alumina surface, is present. Finally, the slightly lower intensities observed for the Mo-extracted catalysts than for the unextracted ones (upper curve in Fig. 7) may be due to the lower reduction degree found in such preparations (cf. Figs. 5a and b).

#### O<sub>2</sub> and NO Chemisorption

In order to compare the O<sub>2</sub> and NO chemisorption capacities of the catalysts all of them were prereduced at a similar degree of reduction ( $\alpha = 0.92$ – $0.95$ ). The irreversible O<sub>2</sub> and NO uptakes on both prereduced Mo-extracted and unextracted Mo/Al<sub>2</sub>O<sub>3</sub> catalysts as a function of the Mo loading are presented in Fig. 8. It is clear that the irreversible NO uptakes on all catalysts are

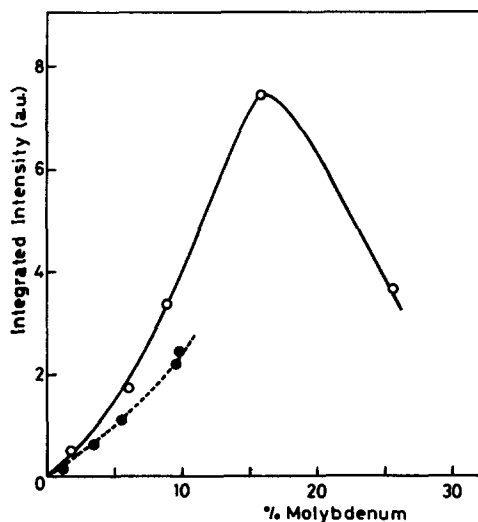


Fig. 7. Integrated intensities of the 1710-cm<sup>-1</sup> band of NO strongly held on prereduced Mo/Al<sub>2</sub>O<sub>3</sub> catalysts as a function of Mo loading. Full points refer to the extracted catalysts.



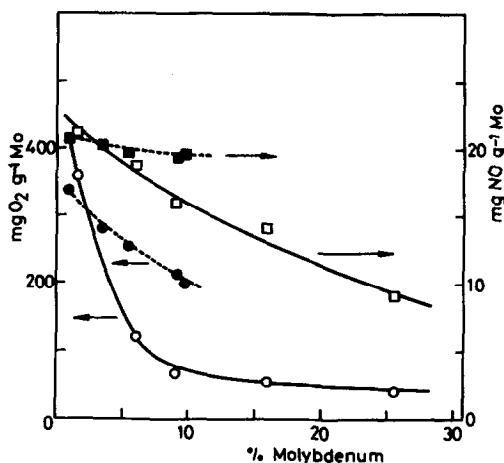


FIG. 8.  $O_2$  and NO irreversible chemisorption amounts on the reduced ( $\alpha = 0.92-0.95$ )  $Mo/Al_2O_3$  catalysts as a function of the Mo loading. Closed symbols refer to extracted catalysts.

much lower than the corresponding  $O_2$  uptakes, a trend known to occur when CO and  $O_2$  were used as probe molecules (33, 34). It is interesting that both NO uptakes generally decrease with increasing Mo loading, but the  $O_2$  uptake decreases more markedly, especially for unextracted catalysts at low Mo loadings. These pronounced decreases in both  $O_2$  and NO uptakes observed for unextracted catalysts indicate that certainly on such catalysts Mo dispersion decreases when Mo loading increases. In the case of the Mo-extracted catalysts, the  $O_2$  uptake also decreases with increasing Mo loading, but less so and more gradually than on unextracted catalysts, while the NO uptake changes only slightly.

For a better comparison, in Table 4 the chemisorption data for  $O_2$  and NO on a few catalysts for both unextracted and Mo-extracted reduced  $Mo/Al_2O_3$  catalysts series expressed as the number ratio of adsorbed molecules to total Mo atoms in the catalysts are summarized. It is evident that, except for the catalyst with very low Mo loading (1.8%), all unextracted catalysts present much lower (2–4 times)  $O_2$  chemisorption capacities than the corresponding Mo-extracted catalysts. This fact indicates that

Mo is poorly dispersed in the high-Mo-loading-unextracted  $Mo/Al_2O_3$  catalysts, since a fraction of Mo easy to reduce is present on the alumina surface in multilayers or in  $MoO_3$  clusters of a few Mo atoms as previously proposed (14). The removal of Mo, predominantly  $Mo[O]$  (polymeric and in multilayer), by ammonia leaves the remaining unextractable Mo fraction stay relatively more dispersed than before extraction, decreasing only slightly with increasing Mo loading. This conclusion is strengthened when the NO/Mo ratios of Table 4 are also compared. Such ratios for Mo-extracted catalysts decrease only slightly as Mo loading increases, i.e., from 0.067 to 0.062, suggesting that such catalysts present no change in dispersion (based on NO adsorption) and very close to that measured for the unextracted 1.8%  $Mo/Al_2O_3$  catalysts. In the latter catalyst, the majority of Mo is probably as a monolayer since both  $O_2/Mo$  and  $NO/Mo$  ratios remain virtually equal before and after Mo extraction. In other words, relative decreases in Mo-extracted and adsorption capacities are similar for the lowest Mo-loading catalyst.

When comparing the chemisorption data of Table 4 with those of literature, the  $O_2/Mo$  ratios found on the unextracted  $Mo/Al_2O_3$  catalysts containing above 6% Mo are comparable with those previously reported on reduced and sulfided catalysts (35, 39). However, the NO/Mo ratios are substantially lower than the corresponding

TABLE 4

Comparison of NO and  $O_2$  Chemisorption Data on Reduced  $Mo/Al_2O_3$  Catalysts

Catalyst	$O_2/Mo$	$O/Mo$	NO/Mo
1.8% $Mo/Al_2O_3$	1.08	2.16	0.068
6.1% $Mo/Al_2O_3$	0.37	0.74	0.060
15.9% $Mo/Al_2O_3$	0.165	0.33	0.045
1.1% $Mo/Al_2O_3^a$	1.02	2.04	0.067
3.5% $Mo/Al_2O_3^a$	0.765	1.53	0.063
9.5% $Mo/Al_2O_3^a$	0.645	1.29	0.062

<sup>a</sup> Extracted catalysts.

values calculated from the chemisorbed amounts of NO determined by the extrapolation of the linear portions of the NO isotherms at zero pressure (40). Note that if we consider the total NO uptake the NO/Mo ratios became larger. For instance, for the H<sub>2</sub>-reduced ( $\alpha = 0.94$ ) 15.9% Mo/Al<sub>2</sub>O<sub>3</sub> catalyst, the NO/Mo ratio obtained by considering irreversible NO uptake is 0.045 whereas by considering total NO uptake it is almost five times higher.

### CONCLUSION

The results presented here indicate that the Mo/Al<sub>2</sub>O<sub>3</sub> catalysts, prepared by the adsorption from solution technique in an excess of solute at pH = 5.70–7.70, contain in their calcined state both Mo[T] and Mo[O] species, but their relative abundance strongly depended on the solute concentration (13, 16) during preparation. With middle (and much more with high) Mo loadings MoO<sub>3</sub> clusters of few Mo atoms were present at the alumina surface. Extraction of Mo multilayers by a 3% ammonia solution gave rise to a highly dispersed Mo phase. TPR profiles until a final temperature of 1000°C of both catalyst series indicated that reduction of Mo ions (Mo[T] as well as Mo[O]) proceeds in two steps: (a) one about 450°C which corresponds to reduction of Mo<sup>6+</sup> to Mo<sup>4+</sup> (as major species), and (b) a second one above 650°C attributable to reduction of ionic Mo sites to metallic Mo (in the Mo-extracted preparations the shift of  $T_1$  and  $T_2$  to higher temperatures indicated a higher Mo[T] concentration than in the unextracted ones). This last finding is supported by the IR spectra of CO chemisorbed on a H<sub>2</sub>-reduced 8.9% Mo/Al<sub>2</sub>O<sub>3</sub> catalyst reduced at 510 and 820°C for 1 h (Fig. 3) which indicated the appearance of metallic Mo first when reduced at 820°C. H<sub>2</sub>-reduced catalysts under standard conditions, viz., 510°C for 1 h, chemisorb NO as (NO)<sub>2</sub> complexes on the ionic Mo sites, mainly Mo<sup>4+</sup> (and possibly Mo<sup>3+</sup> or Mo<sup>2+</sup>). Finally, for the Mo-extracted preparations the higher FWHM of the antisymmetric

band of NO at 1710 cm<sup>-1</sup> reflected a higher participation of the surface inhomogeneities than in the unextracted ones.

### ACKNOWLEDGMENTS

Financial support of this work was done by CAICYT (Spain). One of us (C.V.C.) thanks CONICET (Argentina) for a fellowship.

### REFERENCES

1. Giordano, N., Bart, J. C. J., Vaghi, A., Castellan, S., and Martinotti, G., *J. Catal.* **36**, 81 (1975).
2. De Beer, V. H. J., Van der Aalst, M. J. M., Machiels, C. J., and Schuit, G. C. A., *J. Catal.* **43**, 78 (1976).
3. Mitchell, P. C. H., Martinez, N. P., and Chipunker, P., in "Proceedings, 2nd International Climax Conference on the Chemistry and Uses of Molybdenum" (P. C. H. Mitchell and A. Seaman, Eds.), p. 164. Climax Molybdenum Co., London, 1976.
4. Sonnemans, J., and Mars, P., *J. Catal.* **31**, 209 (1973).
5. Asmolov, G. N., and Krylov, O. V., *Kinet. Katal.* **11**, 847 (1970).
6. Wang, L., and Hall, W. K., *J. Catal.* **77**, 232 (1982).
7. Fierro, J. L. G., Gil, F. J., Lopez Agudo, A., and Rives Arnau, V., in "Proceedings, 8th Ibero-american Symposium on Catalysis," Vol. 1, p. 615. La Rabida, 1982.
8. Iannibello, A., and Mitchell, P. C. H., in "Preparation of Catalysts II" (B. Delmon, P. Grange, P. A. Jacobs, and G. Poncelet, Eds.), p. 469. Elsevier, Amsterdam, 1979.
9. Brunelle, J. P., in "Preparation of Catalysts II" (B. Delmon, P. Grange, J. A. Jacobs, and G. Poncelet, Eds.), p. 211. Elsevier, Amsterdam, 1979.
10. Parfitt, G. D., *Pure Appl. Chem.* **48**, 415 (1976).
11. Parks, C. A., *Chem. Rev.* **65**, 177 (1965).
12. Ashley, J. H., and Mitchell, P. C. H., *J. Chem. Soc. A* 2821 (1961); 2730 (1969).
13. Aulmann, M. A., Siri, G. J., Blanco, M. N., Caceres, C. V., and Thomas, H. J., *Appl. Catal.* **7**, 139 (1983).
14. Gil, F. J., Escudé Castro, A. M., Lopez Agudo, A., and Fierro, J. L. G., *J. Catal.* **90**, 323 (1984).
15. Fierro, J. L. G., Soria, J., and Lopez Agudo, A., *Appl. Catal.* **3**, 117 (1982).
16. Trifiro, F., Forzatti, P., and Villa, P. L., in "Preparation of Catalysts I" (B. Delmon, P. A. Jacobs, and G. Poncelet, Eds.), p. 405. Elsevier, Amsterdam, 1976.
17. Shapiro, K. Ya., Kulakova, V. V., Evstigneeva, E. D., Zuev, V. N., and Nenasheva, N. A., *Russ. J. Inorg. Chem.* **15**, 1155 (1970).

18. Kurtum, G., "Reflectance Spectroscopy." Springer-Verlag, Heidelberg, 1969; Wendlandt, W. W. and Hecht, H. C., "Reflectance Spectroscopy." Interscience, New York, 1966.
19. Thomas, R., Van Oers, E. M., De Beer, V. H. J., Medema, J., and Moulijn, J. A., *J. Catal.* **76**, 241 (1982).
20. Peri, J. B., *J. Phys. Chem.* **72**, 2917 (1968).
21. Sheppard, N., and Nguyen, T. T., *Adv. Infrared Raman Spectrosc.* **5**, 67 (1978).
22. Hair, M. L., "Infrared Spectroscopy in Surface Chemistry." Dekker, New York, 1967.
23. Peri, J. B., *J. Phys. Chem.* **86**, 1615 (1928).
24. Peri, J. B., *Prepr. Amer. Chem. Soc. Div. Pet. Chem.* **23**, 1281 (1978).
25. Yao, H. C., and Rothschild, W. G., in "Proceedings, 4th International Climax Conference on the Chemistry and Uses of Molybdenum" (H. F. Barry and P. C. H. Mitchell, Eds.), p. 31. Ann Arbor, Michigan, 1982.
26. Kazusaka, A., and Howe, R. F., *J. Catal.* **63**, 447 (1980).
27. Hall, W. K., and Millman, W. S., *J. Phys. Chem.* **83**, 427 (1979).
28. Topsøe, N. Y., and Topsøe, H., *J. Catal.* **75**, 354 (1982).
29. Chung, K. S., and Massoth, F. E., *J. Catal.* **64**, 320 (1980).
30. Knözinger, H., and Jeziorowski, H., *J. Phys. Chem.* **82**, 2002 (1978).
31. Okamoto, U., Tomioka, H., Katoh, Y., Imanaka, T., and Teranishi, S., *J. Phys. Chem.* **84**, 1833 (1980).
32. Brown, F. R., Makovsky, L. E., and Rhee, K. H., *J. Catal.* **50**, 162 (1977).
33. Ramakrishnan, N. R., and Weller, S. W., *J. Catal.* **67**, 237 (1981).
34. Bachelier, J., Duchet, J. C., and Cornet, D., *Bull. Soc. Chim. Belg.* **90**, 1301 (1981).
35. Weller, S. W., *Acc. Chem. Res.* **16**, 101 (1983), and references therein.
36. Bodrero, T. A., and Bartholomew, C. H., *J. Catal.* **84**, 145 (1983).
37. Zmierczak, W., Murali Dhar, G., and Massoth, F. E., *J. Catal.* **77**, 432 (1982).
38. Lopez Agudo, A., Gil, F. J., Reyes, P., and Fierro, J. L. G., *Appl. Catal.* **1**, 59 (1981).
39. Delgado, E., Fuentes, G. A., Hermann, C. Kunzmann, G., and Knözinger, H., *Bull. Soc. Chim. Belg.* **93**, 735 (1984).
40. Valyon, J., and Hall, K. W., *J. Catal.* **84**, 216 (1983).